Volume 1 | Number 1 | Jan 2013 | Pages 1–100

Journal of
Materials Chemistry B

Materials for biology and medicine
www.rsc.org/materialsB

ROYAL SOCIETY OF CHEMISTRY

ROYAL SOCIETY OF CHEMISTRY

www.rsc.org/materialsB

Journal Name

ARTICLE TYPE

Effects of hydroxyapatite microparticles morphology on bone mesenchymal stem cell behavior

Hui Yang,[a,b,1] **Huijun Zeng,**[c,1] **Lijing Hao,**[a,b] **Naru Zhao,**[a,b] **Chang Du,***[a,b] **Hua Liao,***[c] **and Yingjun Wang***[a,b]

Understanding the shape effect of hydroxyapatite (HAp) microparticles on cellular behavior is important for enabling kinds of new biological and biomedical applications. However, it's still a challenge to prepare HAp microparticles with different shape but similar physicochemical properties, and then
10 investigate their relationships with cellular behavior. Herein, we developed a novel, facile route to regulate the morphology of HAp microparticles, and investigated the interaction between the particles and bone marrow mesenchymal stem cells (BMSCs). Our results revealed that the shape of HAp has a strong influence on cellular behavior, and the sphere-like particles performed better than that of the rod-like particles. These findings highlight the importance of shape characteristics of HAp microparticles, and
15 may provide new insights for the utility of HAp based materials.

Introduction

HAp possesses excellent biocompatibility because of its chemical composition similarity with the natural bone mineral, and is widely used as artificial bone fillers for repairing bone defects[1].
20 Recently, numerous studies were focused on the interactions between the cells and the HAp nanoparticles with different characteristics (size distribution[2-4], surface chemistry[5]), while the morphology of the particles also played an important role in affecting the cellular behavior [6, 7]. Indeed, some studies have
25 verified the compatibility of HAp particles to cells[3, 8-11], while in some cases they were cytotoxical [7, 12-14]. For example, needle-like HAp particles were biocompatible to BMSCs and promoted cellular proliferation and up-regulated osteogenic differentiation expression level[3]. On the other hand, needle-like HAp inhibited
30 the proliferation of osteoblast. In addition, comparing with spherical and rod-like HAp particles, a higher inflammatory cytokines level was induced[13]. In general, the influence mechanism of HAp particle's shape on cellular behavior is still not clearly understood. Due to the complexity of morphology
35 regulation process of HAp particles[15-18], particles' physicochemical properties[19, 20] and cellular behavior[21], it's still a challenge to prepare HAp microparticles with different shape but similar physicochemical properties, and then investigate their relationships with cellular behavior.
40 Herein, to address this challenge, we developed a novel, facile route to regulate the shape of HAp microparticles through mildly modulating the pH adjustment mode, which is important for ensuring their similar physicochemical properties. BMSCs were co-cultured with the particles and their viability, proliferation and
45 phenotype behavior were investigated in detail. The results indicated that the shape of the particles had a great influence on

cellular behavior, both of them were biocompatible at low concentration condition. In addition, sphere-like particles performed better in promoting the cellular proliferation and
50 osteogenic differentiation. These findings highlight the importance of shape characteristics of HAp microparticles, and may provide new insights for the utility of HAp based materials.

Experimental

Synthesis of HAp microspheres and microrods

55 Unless otherwise stated, all chemicals were of analytical grade reagents and purchased from Guangzhou Chemical Corporation, and used without further purification. For a typical synthesis of HAp microspheres, a solution of diammonium phosphate ($(NH_4)_2HPO_4$, 12 mM, 60 mL) was vigorously stirred and the pH
60 of the solution was adjusted to 6 with HNO_3. Then, calcium nitrate tetrahydrate ($Ca(NO_3)_2 \cdot 4H_2O$, 20 mM) was quickly added into the mixture under vigorous stirring. The pH of the mixture was further adjusted to 5 with HNO_3. As the mixture was homogeneous, 0.9 g sodium citrate was added and the mixture
65 was then stirred for another 10 min to ensure complete dissolving of the reagents. Later, the mixture was transferred into a 100 ml Teflon bottle held in a stainless steel autoclave, sealed and heated at 180 °C for 2 h. As the autoclave cooled to room temperature, the resulting precipitates were washed with de-ionized water for
70 three times, centrifuged and then freeze dried.
For the synthesis of HAp microrods particles, all of the experimental parameters and reagents were the same as that of the HAp microsphere, except the pH adjusting mode. Firstly, when the phosphate source was totally dissolved, the pH of the
75 solution was adjusted to 5 with HNO_3, and then adding calcium source, as the mixture was homogeneous, the pH of the solution

was adjusted to 5 with diluted $NH_3 \cdot H_2O$. After that, 0.9 g sodium citrate was added, and the mixture was stirred for another 10 min. Then the solution was transferred into a 100 ml Teflon bottle held in a stainless steel autoclave, sealed and heated at 180 ^{o}C for 2 h.

5 Being cooled naturally to room temperature, the resulting precipitates were washed with de-ionized water for three times, centrifuged and then freeze dried.

X-ray diffraction analysis

Powder mineralogical phase was analyzed by X-ray diffraction.

10 X-ray diffraction measurements were performed on PANalytical X'Pert PRO X-ray diffractometer with Cu Kα (λ=0.15418 nm) incident radiation, and the XRD data were collected between 10° and 60° in intervals of 0.02° and a scan rate of 1°/min.

Particle size, zeta potential and morphology determination

15 The size distribution of HAp particles were measured by DLS (Zetasizer Nano ZS, Malven Instruments, UK). The value was recorded as the mean of the three measurements. The zeta potential of the particle was also characterized by Zetasizer nano ZS.

20 The morphology of the HAp particles was investigated by field emission scanning electron microscope system (SEM, Nova NanoSEM 430, FEI, Netherlands) at a accelerating voltage of 10 kV.

Fourier transformed infrared analysis

25 Then characteristic bands of the as-prepared samples were studied with Fourier transformed infrared spectrometer (FT-IR, MAGNA 760, Nicolet Instrument, USA). The spectra were collected on KBr discs in the range of 3500-500 cm^{-1}.

Cell culture and seeding

30 Mouse bone mesenchymal stem cells (mBMSCs) were purchased from ATCC (ATCC CRL-12424) and cultured in Dulbecco's Modified Eagle's medium (DMEM) supplemented with 10% FBS and 1% penicillin-streptomycin at 37 ^{o}C in moist environment with 5% CO_2. The medium was replenished every

35 other day and the cells were collected by trypsinization using 0.25% of trypsin-EDTA solution followed by subculture. mBMSCs at population of 3-4 passages were used in following experiments. Cells were seeded onto tissue culture plates with an initial cell seeding density of 1×10^4 cells/cm^2 for all experiments.

40 Cell suspension (1 ml) was initially dropped onto the tissue culture plates and cultured for 24 h, and then certain amount of particles with different morphologies were added into the culture medium. The chemical reagents used for osteogenic differentiation were a mixture of 10 mM β-glycerophosphate, 50

45 μM ascorbic, and 100 nM dexamethasone (all these reagents were purchased from Sigma). After cultured for a certain period, the subsequent measurements at the desired time of intervals were conducted.

Cytotoxicity and cell viability

50 Microparticles were sterilized with autoclaving treatment, and 10 ml DMEM was added into the vial, then the mixture was re-suspended by ultrasonic to ensure an even suspension of HAp particles. After that, the mixture was stored as aqueous suspensions at 4 ^{o}C. The cytotoxicity of the particles to the cells

55 was assessed by measuring LDH activity released from damaged cells into the media. A cytotoxicity detection kitPlus (Roche Applied Sciences) was used as follows: Cells were exposed to the HAp particles in culture medium at the following concentrations: 1000, 500, 200, and 100 μg/ml. Then, 100 μl of cell culture

60 supernatant was removed and mixed with 100 μl LDH assay mixture, which was transferred into a 96 well plate. The high control was prepared by incubating the untreated cells with lyses solution (containing 2% Triton X-100) for 30 min at 37 ^{o}C. After that, 100 μl cell lysate mixed with 100 μl LDH assay mixture in a

65 96 well plate. The cells cultured in growth medium without adding microparticles were treated as low control group, 100 μl supernatant from each sample was transferred to 96-well plates with 100 μl LDH assay mixture. Then the absorbance of the mixtures was measured at 490 nm with a reference wavelength of

70 620 nm (Thermo 3001 Microplate Reader). The cytotoxicity was calculated according to the following equation:

$$\text{Cytotoxicity (\%)} = \frac{A_{\text{experimental group}} - A_{\text{low control}}}{A_{\text{high control}} - A_{\text{low control}}} \times \mathbf{100}\%$$

Cell viability was evaluated with CCK-8 assay (Dojundo,

75 Kumamoto, Japan), it is a kind of higher sensitivity reagent for cell viability assay and has a better reproducibility than MTT (3-(4, 5-dimethylthiazol-2-yl)-2, 5-diphenyltetrazolium bromide)[22]. Cells (10000 cells/cm2) were cultured in 24-well TCPS (tissue culture polystyrene) for 24 h, then certain concentration of

80 microparticles were added, and cultured in a humid atmosphere under 37 ^{o}C and 5% CO2 for 24, 72, and 120 h. Cells seeded on bar TCPS (without HAp particles) was using as negative control. At specific time intervals, the medium was discarded and the mixture composed by 300 μl fresh culture medium and 30 μl

85 CCK-8 solution were added to each well, then the plate was incubated at 37 ^{o}C for 1 h, 100 μl supernatant was transferred into 96-well plate, and the absorbance was analyzed with a microplate reader at 450 nm.

Real time quantitative reverse transcription-polymerase

90 **chainreaction**

mBMSCs at the density of 1×10^4 cells/cm^2 was cultured with the materials for a certain period of time in osteogenic differentiation medium, and then the total RNA was isolated with HiPure Total RNA Kits (Magen, China) following the protocol and subjected

95 to RT with SuperScript^{TM} First-Strand Synthesis System (Promega, U.S.A). The yielded complementary (cDNA) was then subjected to PCR examining gene expression of the alkaline phosphatase (ALP), the alpha 1 chain of type I collagen (ColI), osteocalcin (OC), runx2 and β-actin. The adopted primer

100 sequences were listed in Table 1. The quantitative polymerase chain reaction (qPCR) was conducted with SYBR green assay (Iq supremix, Bio-rad). The gene expressions were quantified with a calculation of $2^{-\Delta\Delta C}$, where C represented the cycle number when an arbitrarily placed threshold was reached, and $\Delta\Delta C$ = sample

105 group($C_{\text{target gene}}$-$C_{\beta\text{-actin}}$) – control group ($C_{\text{target gene}}$-$C_{\beta\text{-actin}}$).

ALP and Collagen staining

The ALP and collagen secreted by the cells was investigated by using BCIP/NBT (KPL, U.S.A) and Sirius Red, respectively. Briefly, after the cells (1×10^4 cells/cm^2) was co-cultured with

the particles for 7 d and 14 d in differentiation medium, the culture medium was removed and the cells was rinsed with PBS for 3 times, then 300 μl BCIP/NBT solution was added to stain for 25 min; The collagen secretion was assessed by Sirius Red[23]
5 (Aladdin), after the cells were rinsed with PBS for 3 times and fixed with PBS solution containing 4% formaldehyde for 30 min, then 500 μl saturated picric acid solution containing 0.1% Sirius red was added and the cells were stained for 3 h. The unbound stain was washed with 0.1 M citric acid solution for 1 h, and then
10 the images were taken.

Uptake experiments with the aid of TEM and flow cytometry

The particles internalized by the cells were characterized by using TEM and Flow cytometry, respectively. The TEM samples were obtained as follows: Cells (1 x 10^4 cells/cm^2) were cultured in
15 culture plate for 24 h, and then 200 μg/ml particles were added into the culture system for a certain period of time. Then the cells were rinsed with PBS for three times and digested with 0.25% trypsin, the cells solution were centrifuged at 125 g for 5 min, and then fixed with the solution (pH=7.4) containing 2%
20 paraformaldehyde, 2.5% glutaraldehyde and 0.15 M Na_3PO_4 for 12 h at 4 ^{o}C. The cells were dehydrated with increasing concentration of ethanol (30%, 50%, 60%, 70%, 80%, 90%, 95%, 100%, 5 min each) and embedded in epoxy resin, the samples with the thickness at about 70 nm were obtained by using a
25 diamond knife, and then collected on 200-mesh copper, viewed by using a TEM (Tecnai G2 spirit twin ,FEI) operating at 80 kV.
To quantify the amount of the particles internalized by the cells, flow cytometry was used. Particles were labelled with FITC[24], Briefly, 20 mg HAp particle and 4 ml 3-
30 aminopropyltriethoxysilane (AMPTES) were mixed with 20 ml ethanol solution, and the mixture reacted at 74 ^{o}C for 3 h. Then 10 mg FITC was added and continued to react for another 6 h at 74 ^{o}C, the FITC labelled particles were dialyzed to remove the unbounded FITC, freeze dried for further use. After the cells (1 x
35 10^4 cells/cm^2) were cultured at tissue plate for 24 h, 200 μg/ml FITC labelled particles were added, as they were co-cultured for 3 h and 24 h, the cells were washed with PBS for 3 times, and then treated with 0.25% trypsin, centrifuged at 125 g for 5 min. The cells pellets were re-suspended in PBS solution and 200 μl
40 cellular suspension was used to quantify the particles' internalization efficiency by the cells with the aid of flow cytometry (Guava easycyte, Millipore).

Statistical analysis

Experiments were repeated three times and results were
45 expressed as means ± standard deviations. CCK-8 assay, LDH assay, RT-PCR and flow cytometry analysis results were evaluated by one way analysis of variance (ANOVA). A comparison between two means was analyzed with Tukey's test with statistical significance set at p<0.05.

50 Table 1 Validated Primer Sequences for Real-time PCR

Gene	Direction	Sequence (5'-3')
ALP	Forward	TGCCTACTTGTGTGGCGTGAA
	Reverse	TCACCCGAGTGGTAGTCACAATG
OC	Forward	AGCAGCTTGGCCCAGACCTA
	Reverse	TAGCGCCGGAGTCTGTTCACTAC
Col I	Forward	ATGCCGCGACCTCAAGATG
	Reverse	TGAGGCACAGACGGCTGAGTA
Runx2	Forward	CACTGGCGGTGCAACAAGA
	Reverse	TTTCATAACAGCGGAGGCATTTC
β-actin	Forward	TGACAGGATGCAGAAGGAGA
	Reverse	GCTGGAAGGTGGACAGTGAG

Results

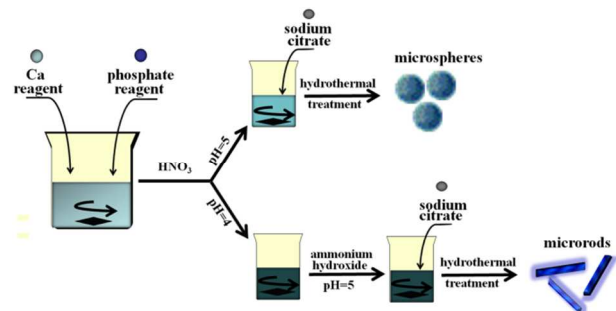### Characterization of microparticles

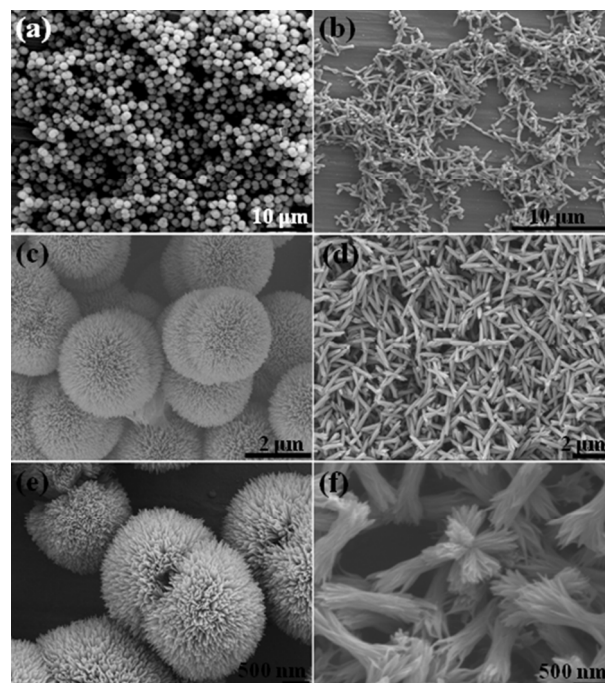55 Figure 1 scheme represented the preparation process of microspheres and microrods.

Figure 2 SEM images of the as-prepared particles. a, c, e) microspheres; b, d, f) microrods

60
The as-prepared particles were characterized with SEM and their morphology was shown in Fig. 2. As we can see, the particles were uniform. The size of the microspheres is about 2-3 μm; The length of the microrods was about 1 μm, and its diameter was
65 about 200 nm. Both particles consisted of nanoscale building units and the microsphere had a much rougher surface than the microrod. The results indicated that the pH adjusting mode could greatly influence the shape of the final products.
To further analyse their physical and chemical properties, XRD,
70 FTIR, size distribution and zeta potential were also investigated. As shown in Fig. 3(a), all of the diffraction peaks could be indexed as hexagonal HAp, and without obvious impurity crystal phase was observed. In addition, the broadening peaks at around

30-40° showed a poor crystalline status and the products were non-stoichiometric HAp. The crystallinity of microsphere particles was higher than that of microrod particles. The infrared spectroscopy of the products was similar (Fig. 3(b)). The
5 characteristic bands at around 1000 and 500 cm⁻¹ were assigned to the vibration of PO_4^{3-} [25], the peak at 3568 cm⁻¹ was ascribed to the vibration of –OH, and the bonds of CO_3^{2-} (among 1400 – 1500 cm⁻¹) [26] also appeared in the spectra. The size distribution analysis was conducted as shown in Fig. 3(c), the average size of
10 the microspheres was 2.83 μm, and the size distribution column indicated slight aggregation phenomenon existence, and the final size distribution was around 1-6 μm. Moreover, the average size of the microrods was 765 nm in length. And the size distribution column showed its size was among 200 nm – 3 μm, which also
15 demonstrated a slight aggregation phenomenon in the system. The zeta potentials of the microspheres and microrods were -14.5 ± 0.6 and -16.9 ± 0.4 mV, respectively.
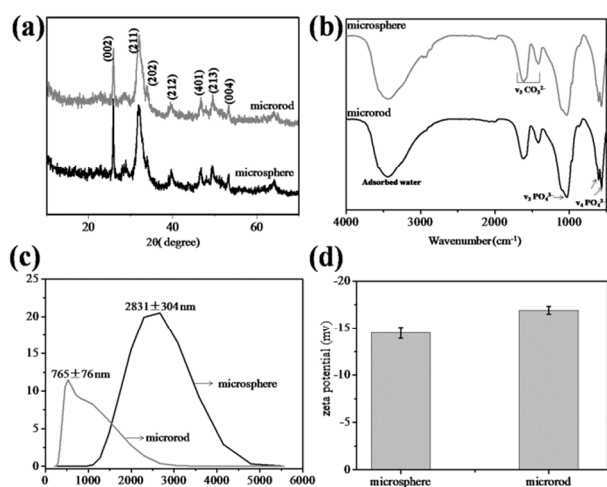

Figure 3 (a) the XRD patterns, (b) the FTIR spectra, (c) the size
20 distribution, (d) the zeta potential of the microspheres and microrods.

Cytokine release after co-culture for 3 and 24h (ELISA)
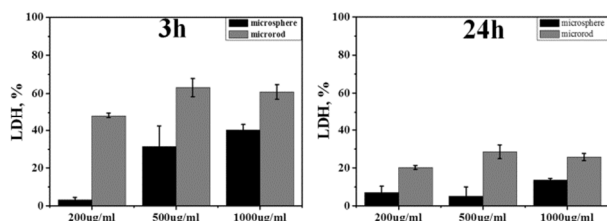

25 Figure 4 Cytotoxicity of HAp microparticles. mBMSCs were incubated with particles at different concentration for 3 h and 24 h. The concentration of the particles was proportion to the cytotoxicity level. The LDH releasing data showed the percentage of related LDH as a fraction of total cellular and
30 released LDH. Value represented the means ± SE, n=3.

As shown in Fig. 4, two kinds of particles with different concentration were co-cultured with the mBMSCs, the LDH releasing level was detected after incubating with cells for 3 h

35 and 24h. The concentration of the particles was proportional to the inflammatory effect. When the particles' concentration exceeded 500 μg/ml, both of the two kinds of particles resulted in obvious cytotoxicity at short interval. With the culture time prolonged, the viability of the cells gradually recovered; As the
40 concentration of the particles was below 200 μg/ml, although the microrods still led to a slight cytotoxicity, the microspheres performed well and no obvious inflammatory effect was observed. Moreover, the cytotoxicity level decreased as the culture time prolonged. Hence, the results indicated the
45 microspheres generated lower cytotoxicity comparing to the microrods particles.
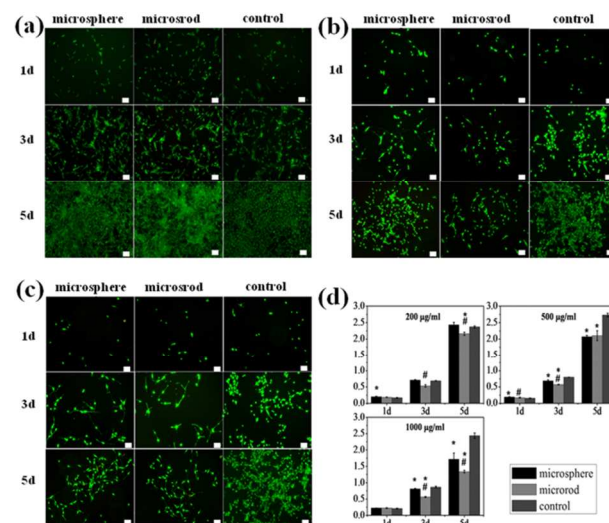
cell viability/proliferation

Figure 5 cellular live/dead staining and proliferation as co-
50 cultured with particles at different concentration. Live/dead staining (a) 200 μg/ml, (b) 500 μg/ml, (c) 1000 μg/ml, and (d) proliferation of mBMSCs. The length of the scale bar is 100 μm.

mBMSCs were treated with HAp microparticles (200, 500 1000
55 μg/ml), and their live/dead and proliferation status were obtained after culture for 1 d, 3 d and 5 d. The results showed that the growth inhibition effect caused by the particles was dose dependent. As the concentration of the particles exceeded 500 μg/ml, an obvious inhibition phenomenon was found for both of the
60 particles. While as the concentration decreased to 200 μg/ml, although the microrods still led to slight cytotoxicity, the microspheres performed well without affecting the viability of the cells. Moreover, inhibition effect for microrods was higher than that of HAp microsphere.
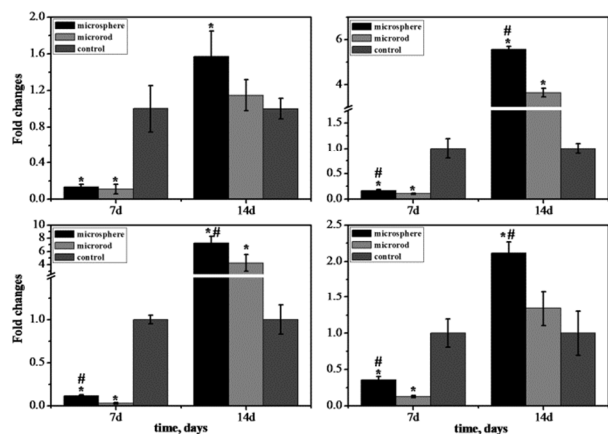
Figure 6 Effects of HAp microparticles (200 μg/ml) on mBMSCs osteogenic differentiation as they were co-cultured for 7 d and 14 d. The cells treated with osteoconductive medium without adding particles serve as a control. These data suggested that both microspheres and microrods inhibited the osteogenic differentiation of the cells at the initial culture period, while they promoted the osteogenic differentiation as co-culture time prolonged to 14 d, especially for microspheres particles. * and # indicate statistical significance compared with the control group and microrods group, respectively.

osteogenic differentiation of mBMSCs

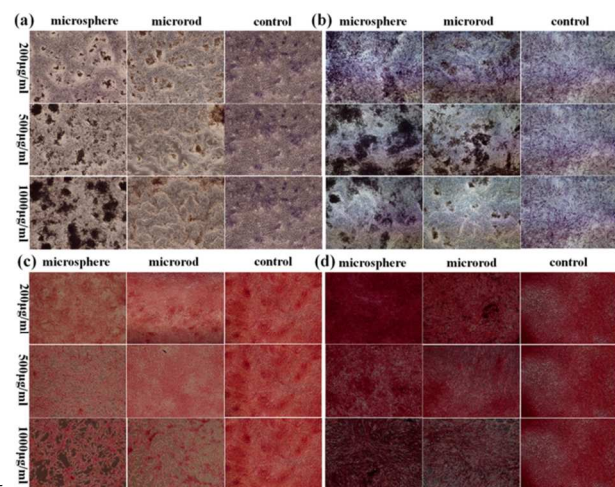***Cultured with the HAp particles with different shape***

Figure 7 ALP staining of mBMSCs after co-cultured with the particles of different concentration for 7 d (a) and 14 d (b); Collagen secreted by mBMSCs as co-cultured with the particles of different concentration for 7 d (c) and 14 d (d). The length of the scale bar is 100 μm.

The cells and particles (200 μg/ml) were co-cultured for 7 d and 14 d in differentiation medium, the relative gene expression level was detected. Compared with the control group, all of the osteoblast-related gene expression level was down regulated for 7 d group. The expression level of ALP for microspheres was similar with that of microrods, and no statistical significant difference existed, however, when compared with other relative gene expression levels, the inhibition effectiveness of microspheres was less than that of microrods. As the culture time prolonged to 14 d, almost all of the osteoblast-related gene expression was up-regulated. And the enhancing effect of

microspheres was still stronger than that of microrods. In addition, when the concentration of the particles was low, the ALP and collagen staining also indicated that the particles inhibited the osteogenic differentiation at the very initial stage (7 d), and then promoted the differentiation process when the culture time prolonged to 14 d. Higher concentration of particles was harmful for the ALP and collagen secretion.

Cells cultured with the supernatant of HAp particles

As the HAp particles could release ions, such as Ca^{2+}, PO_4^{3-}, and even citrate ions. All of these substances might affect the metabolism and differentiation process of the cells [27]. To investigate the remote effects of particles on the development of an osteoblastic phenotype, an experimental approach that avoided direct cell-particle contact was conducted (Figure 8). The cells were cultured with the leach liquor of the HAp, and their concentration was equal to that of the co-culture group treated with particles. As we can see, when the culture time was 7 d, the relative gene expression level was slightly up-regulated, especially for the ALP and OC expression. Moreover, there was no statistically significant difference between microspheres and microrods group. Hence, we concluded that the dissolution of the two kinds of particles has similar promotion effects, while the differentiation inhibition was caused mainly by the cell-particle contact and was particle shape-dependent.
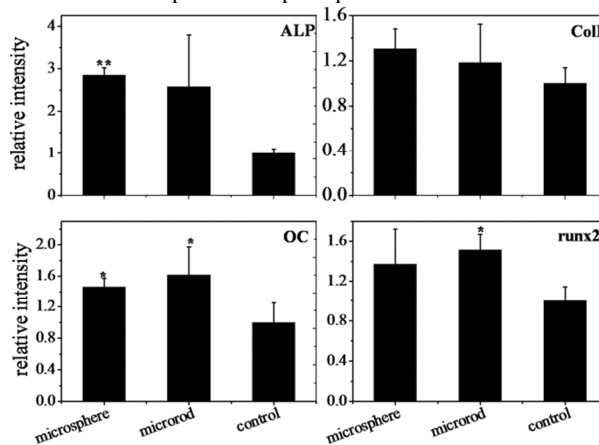

Figure 8 Effect of leaching liquor of HAp with different shape on the osteoblast-related gene expression of mBMSCs. Comparing with the control group, the * and ** indicated p<0.05 and p<0.01, respectively.

Particles internalization by cells

To reveal the inhibition effect caused by the particles, particles internalization by the cell was investigated. As shown in Fig. 9, both of microspheres and microrods could be internalized by the cells. The TEM results indicated that particles entered into the cells after co-culture for 3 h, the particles were uniformly dispersed and no obvious aggregation formed. Moreover, although the size of the microspheres was bigger than that of the microrods, the cells were more prone to internalize microspheres but not microrods particles, and the difference was more obvious as the culture time prolonged to 24h. Hence, comparing to size, particles' shape is a more important factor in affecting the internalization behavior of cells.

Discussion

The shape of materials is closely related to their properties, such as optical, magnetic property and biocompatibility status [28]. Various methods were used for synthesizing materials with complex morphologies. Herein, two kinds of HAp particles were synthesized with the aid of citrate, and the morphology regulation process was achieved through altering the pH adjusting mode. Although the real formation mechanism was still unknown, we speculated that the adding of ammonia water was a key factor. As the addition of alkaline substance in the reaction mixture resulted in the increasing of local degree of supersaturation, and caused the formation of crystal nucleus, and the adsorption of citrate would stabilize them. Therefore, compared with the mixture without adding ammonia water, the nucleation and crystal growth process were boosting, the higher consuming rates of the reaction substance also impaired the possibility of fractal growth, so the microrods but not the microspheres generated. This tiny difference in synthesis process endowed them with similar physical and chemical properties, such as the crystal phase, the composition, size distribution and zeta potential just as shown in Fig. 2.
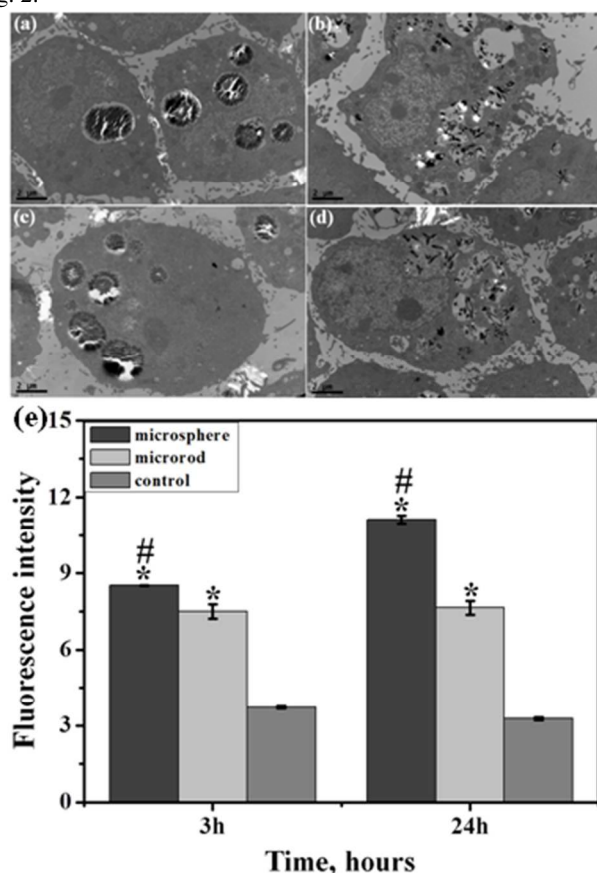

Figure 9 TEM images of cells after the microparticles were internalized as co-cultured for a certain period of time (a) 3 h, microspheres; (b) 3 h, microrods; (c) 24 h, microspheres; (d) 24 h, microrods, and (e) the fluorescence intensity of the cells tested by flow cytometry. The * represented statistical difference between experiment groups and control group, and # meant statistical difference between microspheres and microrods group.

HAp possesses excellent biocompatibility, bioactivity, osteoconductivity and even bone inductivity because of its chemical similarity with the natural bone minerals. Analysis of retrieval calcium phosphate particles demonstrated that the crystal phase, size distribution, shape and the degree of crystallinity influenced the cellular response [4, 13, 29, 30]. Different kinds of calcium phosphate powders (β-TCP, HAp, β-dicalcium pyrophosphate) impaired the rat osteoblast growth in vitro studies under certain conditions [31]. Therefore, the particles releasing from calcium phosphate prostheses might affected the viability of the adjacent osteoblast precursors, compromising the success of bone regeneration [32]. Herein, HAp microspheres and microrods particles were cultured with the mBMSCs, and both of them inhibited the viability of the cells at high dose condition (exceed 500 μg/ml). However, the inhibition effect was greatly decreased as their concentration was lower than 200 μg/ml, especially for that of the microspheres. In addition we found that the osteogenic differentiation process was inhibited at the initial stage (7 d) but promoted as the culture time prolonged to 14 d. However, through investigating the influence of the releasing ions on cell behavior with leaching liquor of HAp particles, we found the leaching liquor of both types of particles promoted the celluar osteogenic differentiation process, and there was no statistically significant difference between the microrod and microsphere groups. The crystallinity of microsphere was higher than that of microrod particles. But the microsphere has a larger specific surface area probably due to its nanoscale crystalline building units. Larger specific surface area can promote the Ca release from microsphere particles, while lower crystallinity is helpful for Ca release from microrod particles. Collectively, the two kinds of particles may have a similar Ca release profile, generating no statistically significant difference between the microrod and microsphere groups when their leaching liquor interacted with the cells. Nevertheless, the possibility of other factors than the shape effect such as the crystallinity and specific surface area cannot be completely ruled out and would be interesting topic for the future study.

Laquerriere P. et al reported that the needle-like HAp caused stronger inflammatory response when cultured with human macrophage comparing to the spherical particles [13]. And the difference in toxicity might associate with membrane damage of cells as they contact with the particles [33]. The concentration related cytotoxicity suggested that cellular particle load was the main cause of cytotoxicity, probably due to the particle internalization by the cells [14, 34]. Although current scientific thought is that, if the nonphagocytotic cells internalized particles through nonspecific endocytosis mode, and the size of the particles exceed 150 nm, they would be excluded from the cellular internalization altogether [35-37]. Stephanie et al reported that the HeLa cells internalized particles exceed 3 μm [34]. Herein, our result was consistent with that of Stephanie in spite of mBMSCs. In addition, the cells showed a higher tendency to internalize the microspheres-like particles though their size was bigger than microrods. Therefore, compared with the size of microparticles, the particles' shape is more prone to affecting the cytotoxicity level. With the growing of the cells, the particles and cells gradually adsorbed together and formed a micro-scaffold, which provided a steady environment for the cells, and the stimulation caused by the particles decreased. Furthermore, the releasing of the calcium ions was helpful for the osteogenic differentiation of the mBMSCs [38]. Hence, after the culture time extended to 14 d, the level of osteoblast-related markers was up-regulated. In addition, compared with the microrods HAp

particles, the up-regulation caused by the microspheres was more efficient. Furthermore, without contacting with the particles, after treatment with the releasing medium of the particles, a up-regulation of the markers happened after co-culturing with the cells for 7 d, that indicated the dissolution of the samples and the releasing calcium ions were helpful for promoting the osteoblast differentiation [39, 40].

Conclusions

We have shown that cellular behavior can be regulated by HAp particles, and the morphology of the particles has a significant influence on cellular behavior. Although both of the microsphere and microrod inhibited the proliferation of the cells at a high dose condition, the inhibition effect decreased or even became negligible with their concentration decreasing. Moreover, the HAp microsphere performed better than that of the microrod particles for promoting osteogenic differentiation of mBMSCs. These findings highlight the importance of shape characteristics of HAp microparticles, and may provide new insights for the utility of HAp based materials.

Acknowledgement

Notes

a School of Materials Science and Engineering, South China University of Technology, Guangzhou, China. E-mail: duchang@scut.edu.cn
b National Engineering Research Center for Tissue Restoration and Reconstruction, Guangzhou, China. Email: imwangyj@163.com
c Department of Anatomy, Key Laboratory of Construction and Detection of Guangdong Province, South Medical University, Guangzhou, hua-liao@163.com
1 These authors contributed equally to this work
† Electronic Supplementary Information (ESI) available: details of any supplementary information available should be included here. See DOI: 10.1039/b000000x/

References

1. K. J. L. Burg, S. Porter and J. F. Kellam, *Biomaterials*, 2000, **21**, 2347-2359.
2. J. S. Sun, H. C. Liu, W. Hong‐Shong Chang, J. Li, F. H. Lin and H. C. Tai, *J Biomed Mater Res*, 1998, **39**, 390-397.
3. Y. Huang, G. Zhou, L. Zheng, H. Liu, X. Niu and Y. Fan, *Nanoscale*, 2012, **4**, 2484-2490.
4. T. Lange, A. F. Schilling, F. Peters, J. Mujas, D. Wicklein and M. Amling, *Biomaterials*, 2011, **32**, 4067-4075.
5. L. Chen, J. M. Mccrate, J. C. Lee and H. Li, *Nanotechnology*, 2011, **22**, 105708.
6. J. Xu, K. A. Khor, J. Sui, J. Zhang and W. N. Chen, *Biomaterials*, 2009, **30**, 5385-5391.
7. Z. Xu, C. Liu, J. Wei and J. Sun, *Journal of Applied Toxicology*, 2012, **32**, 429-435.
8. Y. Cai, Y. Liu, W. Yan, Q. Hu, J. Tao, M. Zhang, Z. Shi and R. Tang, *J Mater Chem*, 2007, **17**, 3780-3787.
9. H. Wang, Y. Li, Y. Zuo, J. Li, S. Ma and L. Cheng, *Biomaterials*, 2007, **28**, 3338-3348.
10. V. V. Sokolova, I. Radtke, R. Heumann and M. Epple, *Biomaterials*, 2006, **27**, 3147-3153.
11. M. Jordan and F. Wurm, *Methods*, 2004, **33**, 136-143.
12. S. B. Goodman, T. Ma, R. Chiu, R. Ramachandran and R. Lane Smith, *Biomaterials*, 2006, **27**, 6096-6101.
13. P. Laquerriere, A. Grandjean-Laquerriere, E. Jallot, G. Balossier, P. Frayssinet and M. Guenounou, *Biomaterials*, 2003, **24**, 2739-2747.
14. M. Motskin, D. Wright, K. Muller, N. Kyle, T. Gard, A. Porter and J. Skepper, *Biomaterials*, 2009, **30**, 3307-3317.
15. B. Viswanath and N. Ravishankar, *Biomaterials*, 2008, **29**, 4855-4863.
16. B. Xie and G. H. Nancollas, *Proceedings of the National Academy of Sciences*, 2010, **107**, 22369.
17. C. M. Zhang, Z. Y. Cheng, P. P. Yang, Z. H. Xu, C. Peng, G. G. Li and J. Lin, *Langmuir*, 2009, **25**, 13591-13598.
18. H. Coelfen, *Nat Mater*, 2010, **9**, 960-961.
19. G. Yin, Z. Liu, J. Zhan, F. Ding and N. Yuan, *Chem Eng J*, 2002, **87**, 181-186.
20. C. Stotzel, F. A. Muller, F. Reinert, F. Niederdraenk, J. E. Barralet and U. Gbureck, *Colloid Surface B*, 2009, **74**, 91-95.
21. F. X. Long, *Nature Reviews Molecular Cell Biology*, 2012, **13**, 27-38.
22. Y. Ling, K. Wei, Y. Luo, X. Gao and S. Zhong, *Biomaterials*, 2011, **32**, 7139-7150.
23. L. C. Junqueira, G. Bignolas and R. Brentani, *The Histochemical journal*, 1979, **11**, 447-455.
24. Y. Yuan, C. Liu, J. Qian, J. Wang and Y. Zhang, *Biomaterials*, 2010, **31**, 730-740.
25. S. Koutsopoulos, *J Biomed Mater Res*, 2002, **62**, 600-612.
26. R. N. Panda, M. F. Hsieh, R. J. Chung and T. S. Chin, *J Phys Chem Solids*, 2003, **64**, 193-199.
27. S. Maeno, Y. Niki, H. Matsumoto, H. Morioka, T. Yatabe, A. Funayama, Y. Toyama, T. Taguchi and J. Tanaka, *Biomaterials*, 2005, **26**, 4847-4855.
28. M. Johnsson, C. F. Richardson, J. D. Sallis and G. H. Nancollas, *Calcified Tissue Int*, 1991, **49**, 134-137.
29. G. Balasundaram, M. Sato and T. J. Webster, *Biomaterials*, 2006, **27**, 2798-2805.
30. C. Wang, Y. Duan, B. Markovic, J. Barbara, C. R. Howlett, X. Zhang and H. Zreiqat, *Biomaterials*, 2004, **25**, 2507-2514.
31. J. S. Sun, Y. H. Tsuang, C. J. Liao, H. C. Liu, Y. S. Hang and F. H. Lin, *J Biomed Mater Res*, 1997, **37**, 324-334.
32. L. Saldana, S. Sanchez-Salcedo, I. Izquierdo-Barba, F. Bensiamar, L. Munuera, M. Vallet-Regi and N. Vilaboa, *Acta Biomater*, 2009, **5**, 1294-1305.
33. E. Evans and E. Clarke-Smith, *Clinical materials*, 1991, **7**, 241-245.
34. S. E. Gratton, P. A. Ropp, P. D. Pohlhaus, J. C. Luft, V. J. Madden, M. E. Napier and J. M. DeSimone, *Proceedings of the National Academy of Sciences*, 2008, **105**, 11613-11618.
35. S. D. Conner and S. L. Schmid, *Nature*, 2003, **422**, 37-44.
36. B. D. Chithrani, A. A. Ghazani and W. C. Chan, *Nano Lett*, 2006, **6**, 662-668.
37. D. J. Gary, N. Puri and Y.-Y. Won, *J Control Release*, 2007, **121**, 64-73.

38. R. L. Duncan, K. A. Akanbi and M. C. Farach-Carson, in *Seminars in nephrology*, 1998, pp. 178-190.

39. S. Ma, Y. Yang, D. L. Carnes, K. Kim, S. Park, S. H. Oh and J. L. Ong, *The Journal of oral implantology*, 2005, **31**, 61-67.

5 40. A. Barradas, H. A. Fernandes, N. Groen, Y. C. Chai, J. Schrooten, J. van de Peppel, J. P. van Leeuwen, C. A. van Blitterswijk and J. de Boer, *Biomaterials*, 2012, **33**, 3205-3215.